



HAL
open science

On the relationship between oxidation state and temperature of volcanic gas emissions

Yves Moussallam, Clive Oppenheimer, Bruno Scaillet

► To cite this version:

Yves Moussallam, Clive Oppenheimer, Bruno Scaillet. On the relationship between oxidation state and temperature of volcanic gas emissions. *Earth and Planetary Science Letters*, 2019, 520, pp.260-267. 10.1016/j.epsl.2019.05.036 . insu-02157512

HAL Id: insu-02157512

<https://insu.hal.science/insu-02157512v1>

Submitted on 18 Jun 2019

HAL is a multi-disciplinary open access archive for the deposit and dissemination of scientific research documents, whether they are published or not. The documents may come from teaching and research institutions in France or abroad, or from public or private research centers.

L'archive ouverte pluridisciplinaire **HAL**, est destinée au dépôt et à la diffusion de documents scientifiques de niveau recherche, publiés ou non, émanant des établissements d'enseignement et de recherche français ou étrangers, des laboratoires publics ou privés.



Distributed under a Creative Commons Attribution - NonCommercial - NoDerivatives 4.0 International License

1 On the relationship between oxidation state and temperature of 2 volcanic gas emissions

3 **Yves Moussallam^{1,2}, Clive Oppenheimer¹, Bruno Scaillet³.**

4 ¹*Department of Geography, University of Cambridge, Downing Place, Cambridge, CB2 3EN, UK*

5 ²*Laboratoire Magmas et Volcans, Univ. Blaise Pascal – CNRS – IRD, OPGC, 63000 Clermont-Ferrand, France*

6 ³*ISTO, 7327 Université d'Orléans-CNRS-BRGM, 1A rue de la Férollerie, 45071 Orléans cedex 2, France*

7

8 Corresponding author: Yves Moussallam; yves.moussallam@ird.fr

9 **Keywords:** oxygen fugacity; volcanic degassing; early Earth; redox; great oxidation event.

10

11 **ABSTRACT**

12 The oxidation state of volcanic gas emissions influences the composition of the exosphere and
13 planetary habitability. It is widely considered to be associated with the oxidation state of the
14 melt from which volatiles exsolve. Here, we present a global synthesis of volcanic gas
15 measurements. We define the mean oxidation state of volcanic gas emissions on Earth today
16 and show that, globally, gas oxidation state, relative to rock buffers, is a strong function of
17 emission temperature, increasing by several orders of magnitude as temperature decreases. The
18 trend is independent of melt composition and geodynamic setting. This observation may
19 explain why the mean oxidation state of volcanic gas emissions on Earth has apparently
20 increased since the Archean, without a corresponding shift in melt oxidation state. We argue
21 that progressive cooling of the mantle and the cessation of komatiite generation should have
22 been accompanied by a substantial increase of the oxidation state of volcanic gases around the
23 onset of the Great Oxidation Event. This may have accelerated or facilitated the transition to
24 an oxygen-rich atmosphere. Overall, our data, along with previous work, show that there is no
25 single nor simple relationships between mantle, magmas and volcanic gas redox states.

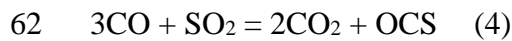
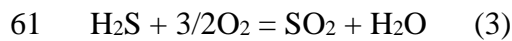
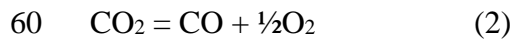
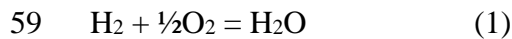
26 I. INTRODUCTION

27 The secondary atmospheres of planetary bodies form and evolve by degassing of volatiles from
28 their interiors (e.g., Kasting, 1993; Elkins-Tanton, 2008; Hirschmann and Dasgupta, 2009).
29 The oxidation state of these emissions strongly influences that of the planet's exosphere,
30 dictating its habitability (e.g., Gaillard and Scaillet, 2014; Kasting et al., 2003). On Earth,
31 several lines of evidence suggest that both atmosphere and ocean were oxygen poor during the
32 Archean (e.g., Bekker et al., 2004; Canfield et al., 2000; Farquhar et al., 2007), prior to the
33 Great Oxidation Event (between 2.45 and 2.22 Ga ago) (e.g., Canfield, 2005). It has been
34 argued that a change in the oxidation state of volcanic gas emissions during this period might
35 have played a role in the rapid oxidation of the atmosphere (e.g., Kasting et al., 1993; Holland,
36 2002; Kump and Barley, 2007; Halevy et al., 2010; Gaillard et al., 2011). The underlying
37 processes for such a change remain unclear, however, especially given the lack of evidence for
38 more reducing conditions in the Archean mantle (e.g., Berry et al., 2008; Canil, 1997, 2002;
39 Rollinson et al., 2017).

40 A first step towards understanding the evolution of volcanic gas oxidation state through time
41 is to constrain the oxidation state of volcanic gas emissions on Earth today. Surprisingly, this
42 quantity and its associated natural variability, have not hitherto been constrained. Direct
43 sampling of volcanic gases has been practised for more than a century, often using tubing
44 inserted into vents to avoid or limit air contamination. Much of the resulting analytical data
45 pertains to point-source fumarole emissions (e.g., Symonds et al., 1994). Latterly, field
46 spectroscopy (e.g., Mori et al., 1993) and electrochemical sensing (e.g., Shinohara, 2005) have
47 facilitated measurement of emissions, notably from open vents (characterized by a magma-air
48 interface), where the volcanic gases are already substantially diluted in air. The wealth of data
49 now available permits investigation of the distribution of oxidation state of volcanic gases
50 emitted to the global atmosphere.

51 II. METHOD

52 We compiled a global dataset of high temperature ($\geq 600^\circ\text{C}$) volcanic gases, for which gas-rock
 53 or gas-fluid interactions are minimal (Giggenbach, 1996; Symonds et al., 2001). Data presented
 54 in this paper are provided in the **Supplementary Information** (**Tables S1** and **S2** together with
 55 references). Following established methodology (e.g., Giggenbach, 1980, 1987; 1996; Ohba et
 56 al., 1994; Chiodini and Marini, 1998; Moretti et al., 2003; Moretti and Papale, 2004; Aiuppa
 57 et al., 2011), the oxygen fugacity (fO_2) of volcanic gases was calculated using gas-phase redox
 58 couples that can be expressed by reactions involving oxygen such as:



63 Those can then be translated in terms of fO_2 by introducing the equilibrium constant K ,
 64 considering that, at near atmospheric pressure, the fugacity of a gas is equal to its partial
 65 pressure and using published thermodynamic constants (Chase 1998; Stull et al., 1969):

$$66 \quad \log \frac{H_2}{H_2O} = -\frac{12707}{T} + 2.548 - \frac{1}{2} \log fO_2 \quad (5)$$

$$67 \quad \log \frac{CO_2}{CO} = \frac{14775}{T} - 4.544 + \frac{1}{2} \log fO_2 \quad (6)$$

$$68 \quad \log \frac{SO_2}{H_2S} = \frac{27377}{T} - 3.986 + \frac{3}{2} \log fO_2 - \log fH_2O \quad (7)$$

$$69 \quad \log P = \frac{-15386.45}{T} + 9.24403 - \log \left(\left(\frac{x_{CO}}{x_{CO_2}} \right)^2 \left(\frac{x_{CO}}{x_{OCS}} \right) x_{SO_2} \right) \quad (8)$$

70 Where the pressure (P) and fugacities (f) are in bars and the temperature (T) is in Kelvin. Given
 71 two redox couples, the oxygen fugacity and equilibrium temperature can be calculated.
 72 Alternatively, if the gas temperature is known (i.e. measured by thermocouple at the vent) the
 73 oxygen fugacity can be determined with only one redox couple. Detailed examples of each

74 calculation method are given in the **Supplementary Information**. When using equation (8), we
 75 assume gas emissions have equilibrated to atmospheric pressure.

76

77 Here, we define the oxidation state of a volcanic gas mixture as the deviation (in log units) of
 78 the oxygen fugacity (fO_2) of the gas mixture relative to a mineral redox buffer at the
 79 corresponding temperature. We use the Quartz-Fayalite-Magnetite (QFM) mineral redox
 80 buffer as reported in Frost, (1991) throughout the text.

81 **Detailed examples of gas oxygen fugacity and equilibrium temperature calculations**

82 Here we elaborate on each calculation method used in this study. We take the example of
 83 volcanic gases measured in 1994 from the then active lava dome of Merapi volcano
 84 (Indonesia), in the course of the fifth International Association of Volcanology and Chemistry
 85 gas workshop (Giggenbach et al., 2001). Gases were collected directly at the vent (Gendol
 86 fumarole) and had an exit temperature of 803°C. Proportions (median of six analyses) of H₂O,
 87 CO₂, SO₂, CO, H₂S and H₂ gases were found to be 88.7, 5.56, 0.98, 0.0235, 0.13 and 0.5 mol%,
 88 respectively (Giggenbach et al., 2001). We focus on this analysis because species involved in
 89 three redox couples were measured along with gas emission temperature (the temperature at
 90 which gases are emitted at the fumarole vent). This allows us to demonstrate calculation of gas
 91 oxidation state in various ways, pertinent when fewer redox couples are constrained (most other
 92 analyses in the database only permit one or two calculation methods).

93

94 **The H₂/H₂O and T method**

95 Using the H₂/H₂O molar ratio and the gas emission temperature we can calculate the oxygen
 96 fugacity following **equation 5**, which can be re-arranged as follows:

$$97 \log fO_2 = -2\left(\log \frac{H_2}{H_2O} + \frac{12707}{T} - 2.548\right) \quad (9)$$

98 For an emission temperature of 1076.15°K (803°C) and an H₂/H₂O molar ratio of 0.0056
 99 (0.5/88.7) the calculated log*f*O₂ is -14.02.

100 To express the gas oxidation state as a deviation from the QFM buffer we calculate the log*f*O₂
 101 of the QFM buffer at the corresponding temperature (803°C) and pressure (1 bar) using the
 102 following equation (Frost, 1991):

$$103 \quad \log f O_2 = \frac{A}{T} + B + \frac{C(P-1)}{T} \quad (10)$$

104 Given values for parameters A, B and C of -25096.3, 8.735 and 0.11, respectively, we calculate
 105 that log*f*O₂ of the QFM buffer at 1076.15°K and 1 bar is equal to -14.59.

106 Using the H₂/H₂O and *T* method, the relative oxidation state is given by the difference between
 107 the two values, i.e., QFM+0.56 log units.

108

109 The H₂S/SO₂ and *T* method

110 Using the H₂S/SO₂ ratio and the gas emission temperature we can calculate the oxygen fugacity
 111 following **equation 7** which can be re-arranged as follows:

$$112 \quad \log f O_2 = \frac{2}{3} \left(\log \frac{SO_2}{H_2S} - \frac{27377}{T} + 3.986 + \log f H_2O \right) \quad (11)$$

113 The value of *f*H₂O used here is 0.887 given that, at 1 bar, the fugacity of a gas is equal to its
 114 partial pressure and that $P(H_2O) = (P_{tot} \times n_{H_2O})/n_{tot} = [(1 \text{ bar})(0.887n_{tot})]/(n_{tot}) = 0.887 \text{ bar}$
 115 (where *P* is the pressure in bar and *n_i* the amount specie *i* in mol%) .

116 For an emission temperature of 1076.15°K (803°C) and for an SO₂/H₂S ratio of 7.54
 117 (0.98/0.13) the calculated log*f*O₂ is -13.75.

118 Using the H₂S/SO₂ and *T* method, the relative oxidation state is QFM+0.83 log units.

119

120 The H₂/H₂O and H₂S/SO₂ method

121 Using **equations 9 and 11** and using the parameters for H₂, H₂O, SO₂, H₂S and *f*H₂O defined
 122 previously provides two equations with two unknowns:

$$123 \quad \log fO_2 = -2\left(-2.248 + \frac{12707}{T} - 2.548\right) \quad (12)$$

124 and

$$125 \quad \log fO_2 = \frac{2}{3}\left(0.877 - \frac{27377}{T} + 3.986 - 0.052\right) \quad (13)$$

126 Solving these equations yields an equilibrium temperature of 1122°K (849°C) for a $\log fO_2$ of
 127 -13.06. Using [equation 10](#) to calculate the $\log fO_2$ of the QFM buffer at the corresponding
 128 temperature gives a $\log fO_2$ of -13.64 for QFM. Hence combining H₂/H₂O and H₂S/SO₂ yields
 129 an oxidation state of QFM+0.57 log units.

130

131 The H₂S/SO₂ and CO/CO₂ method

132 Using [equation 11](#), and re-arranging [equation 6](#) as follows:

$$133 \quad \log fO_2 = 2\left(\log \frac{CO_2}{CO} - \frac{14775}{T} + 4.544\right) \quad (14)$$

134 We can then use the parameters for CO₂, CO, SO₂, H₂S and fH_2O defined previously to write
 135 two equations with two unknowns:

$$136 \quad \log fO_2 = \frac{2}{3}\left(0.877 - \frac{27377}{T} + 3.986 - 0.052\right) \quad (15)$$

137 and

$$138 \quad \log fO_2 = 2\left(2.3739 - \frac{14775}{T} + 4.544\right) \quad (16)$$

139 Solving these equations yields an equilibrium temperature of 1063°K (790°C) for a $\log fO_2$ of
 140 -13.96. Using [equation 10](#) to calculate the $\log fO_2$ of the QFM buffer at the corresponding
 141 temperature gives a $\log fO_2$ of -14.87 for QFM. Hence using the CO/CO₂ and H₂S/SO₂ method
 142 the oxidation state is QFM+0.56 log units.

143

144 The CO₂-CO-OCS-SO₂ method

145 For this example, we cannot use the Merapi gas composition as OCS was not reported. We use
 146 instead the composition of the gas emitted during passive degassing from the lava lake of

147 Erebus volcano (Antarctica) (Peters et al., 2014). In this case, neither H₂ nor H₂S were
 148 measured, but equilibrium conditions can still be constrained owing to measurement of OCS.
 149 Molar proportions of H₂O, CO₂, SO₂, CO, HCl, HF, OCS were 58, 38.4, 1, 1.7, 0.7, 1.3 and
 150 0.009 mol%, respectively.

151

152 Using the CO/CO₂ and CO/OCS mixing ratios we can calculate the equilibrium temperature
 153 following equation 8, rearranging as follows:

$$154 \quad T = \frac{-15386.45}{\log P - 9.24403 + \log \left(\left(\frac{x_{CO}}{x_{CO_2}} \right)^2 \left(\frac{x_{CO}}{x_{OCS}} \right) x_{SO_2} \right)} \quad (16)$$

155 Given a XSO₂ of 0.01, a CO/CO₂ molar ratio of 0.043, a CO/OCS molar ratio of 192 and
 156 assuming equilibration at atmospheric pressure (~0.6 bar at Erebus) yields an equilibrium
 157 temperature of 1292 K (1019 °C).

158 To determine the oxygen fugacity, we then use **equation 16**. Given a CO₂/CO ratio of 22.9 and
 159 an equilibrium temperature of 1292 K yields a logfO₂ of -11.13. Using equation 3 to calculate
 160 the logfO₂ of the QFM buffer at the corresponding temperature gives a logfO₂ of -10.69 for
 161 QFM. Hence using the CO₂-CO-OCS method the oxidation state is QFM-0.44 log units.

162

163 **Sensitivity of oxygen fugacity and equilibrium temperature determinations to**
 164 **instrumental and calculation methods**

165 In cases where two redox couples and the emission temperature have been measured, we can
 166 calculate the equilibrium temperature (the temperature at which the gas mixture was last in
 167 equilibrium) as recorded by the gas redox couples and compare it with the emission
 168 temperature (the temperature at which gases are emitted from the vent) as measured in the field
 169 by thermocouples (**Fig. S1**). This shows that gas equilibrium and emission temperatures are
 170 correlated and that, in most cases, the gas last equilibrated at the temperature at which it entered

171 the atmosphere. Fig. S2 shows that the differences between computed gas oxidation state made
172 using either the calculated equilibrium temperature (based on two redox couples) or the
173 measured emission temperature (and one redox couple) are negligible.

174

175 As shown above, the choice of calculation method can affect the calculated value of $\log f_{\text{O}_2}$.
176 Using the Merapi gas example, the calculated oxygen fugacity varies from QFM+0.56 to
177 QFM+0.83 while the calculated equilibrium temperature varies from 790 to 849°C (compared
178 with a measured emission temperature of 803°C). A very conservative estimate of the error
179 associated with the calculation method would therefore be of ± 0.3 log units of the calculated
180 $\log f_{\text{O}_2}$ and of $\pm 50^\circ\text{C}$ on the calculated equilibrium temperature. If we consider, too, that the
181 gas ratio measurements themselves have reported errors typically of $\pm 10\%$ this contributes an
182 error of about ± 0.15 log units on the calculated $\log f_{\text{O}_2}$ (e.g., Moussallam et al., 2017, 2018).
183 Treating these errors sources as independent (a conservative assumption) yields our confidence
184 interval of ± 0.45 log units on the computed $\log f_{\text{O}_2}$.

185

186 One assumption made in all presented calculation is that the oxidation state of the volcanic
187 gases has equilibrated to atmospheric pressure. This is reasonable given that hot volcanic gases
188 will equilibrate very rapidly, at least at temperatures above 800 °C (Gerlach, 2004; Martin et
189 al., 2006).

190

191 **III. RESULTS**

192 Two broad types of observations were used in this study: sensing of the airborne emissions
193 from open-vent volcanoes, and samples collected directly at fumarole vents. We first consider
194 measurements of air-diluted plumes by calculating the equilibrium conditions for reported
195 compositions (Fig. 1A). Persistent degassing dominates the total volcanic volatile flux to the

196 atmosphere (Shinohara, 2013) but detailed gas composition measurements remain sparse, with
197 volcanoes shown in Fig. 1A contributing about a third of the estimated global total volcanic
198 SO₂ outgassing on Earth over the period 2005–2015 (Carn et al., 2017). We identify a strong
199 correlation between the equilibrium temperature – the final temperature at which the gases
200 were equilibrated (Giggenbach, 1987), unperturbed by mixing with the atmosphere (Aiuppa et
201 al., 2011; Martin et al., 2009) – and gas oxidation state (expressed here as the difference, in log
202 units, from the QFM redox buffer (Frost, 1991). A striking pattern emerges: globally, gases
203 recording high equilibrium temperature are more reduced relative to the buffer, while gases
204 with lower equilibrium temperature are more oxidized. Such a pattern is to be expected if
205 considering a single gas mixture (e.g., Giggenbach, 1987; Ohba et al., 1994) as high
206 temperature will favour the reduced state in most redox reactions (e.g., Ottonello et al., 2001;
207 Moretti and Ottonello, 2005), but the fact that globally, unrelated volcanic gases – emitted by
208 volcanoes in distinct geodynamic settings and with distinct melt composition – conform to a
209 single trend is surprising.

210

211 We consider next high-temperature volcanic gases sampled directly, at fumaroles or via
212 skylights in lava tubes close to the vent, and analysed in the laboratory (e.g., Symonds et al.,
213 1994) (Fig. 1B). In this case, emission temperatures were measured *in situ* by thermocouples,
214 and we have calculated corresponding oxidation states from the reported gas compositions.
215 Despite the marked differences in measurement techniques compared with the air-diluted
216 plume dataset (Fig. 1A), we identify a very similar relationship between gas temperature and
217 oxidation state. Worldwide, gases emitted at high temperatures are more reduced relative to the
218 QFM redox buffer than gases emitted at lower temperatures. That two independent datasets
219 display the same trend suggests a fundamental global relationship between the oxidation state
220 and temperature of volcanic gases.

221

222 **Fig. 2** shows the same data as **Fig. 1** but classed according to the instrumental method and to
223 the method used to calculate the oxygen fugacity and, where applicable, the equilibrium
224 temperature. It is clear from these figures that the inverse correlation observed between the gas
225 oxidation state and emission or equilibrium temperature is well-defined regardless of the
226 methodology used to acquire the gas compositional data or the computation method used.

227

228 To estimate the mean oxidation state of volcanic gases on Earth at present, we draw on a
229 synthesis of a decade of satellite measurements of SO₂ emissions (Carn et al., 2017). For each
230 volcano represented both in this dataset and our own, we ascribe a mean oxidation state to the
231 gas. We then weight each volcano's output to the atmosphere according to its SO₂ flux, leading
232 to an estimate of the mean relative oxidation state of volcanic gas emissions on Earth today of
233 QFM+1.0 (**Fig. 3**). About 80% of observed high-temperature gases fall within one log unit of
234 this value.

235

236 **IV. DISCUSSION**

237 Further inspection of **Fig. 1** reveals a lack of any systematic differences between arc, rift and
238 hot-spot volcanoes at comparable temperature (notwithstanding limited overlap). This is in
239 stark contrast to the observed variation in the oxidation state of the corresponding lavas, and
240 inferred oxidation states of their mantle sources: arc volcanoes are associated with more
241 oxidised lavas sourced from more oxidised regions of the mantle than hotspot and rift
242 volcanoes (e.g., Carmichael, 1991; Frost and McCammon, 2008). We also find no relationship
243 between gas oxidation state and composition (mafic-intermediate-silicic) of the associated
244 magma.

245

246 For as long as they remain in the magma, in direct equilibrium with the melt, volcanic gases
247 will have an oxidation state at equilibrium with that melt (e.g., Moretti et al., 2003; Moretti and
248 Papale, 2004). Our observations, however, imply that, to first order, the oxidation state of
249 volcanic gases is mostly decoupled from that of the melts from which they originate. Further,
250 neither the oxidation state of the mantle source region nor the melts produced determines the
251 oxidation state of the associated volcanic gas emissions to the atmosphere.

252

253 The global relationship between gas temperature and oxygen fugacity (fO_2) is shown in Fig.
254 4A. It appears that volcanic gases do not follow a rock redox buffer involving Fe as previously
255 suggested based on data from Kīlauea (Gerlach, 1993). Instead, the global temperature
256 dependence follows the empirical relation:

$$257 \log(fO_2) = -19100 \left(\frac{1}{T} \right) + 4 \quad (17)$$

258 (where T is the temperature in K).

259 We hypothesize that the underlying mechanism is closed-system cooling of the gas, a process
260 invoked from consideration of gas analyses made at Erebus and Kilauea volcanoes (Burgisser
261 et al., 2012; Oppenheimer et al., 2018). As magmatic gas ascends to the surface and expands it
262 cools unless heat is transferred rapidly enough from melt to gas. Accordingly, the gas mixture
263 will re-equilibrate so that its oxidation state is consistent with its internal temperature. The
264 magmatic gas no longer maintains chemical or thermal equilibrium with the surrounding melt.

265

266 Fig. 4A shows the computed oxidation state for closed-system (gas-only) cooling of three
267 representative gas mixtures, indicating a close fit to the observations. In order to assess how
268 much cooling of the volcanic gases has taken place between their escape from the melt and
269 their last retained equilibrium temperature we conducted a review of melt temperature
270 estimates from the literature. The dataset is presented in the supplementary information, Table

271 S4 and in Fig. 5. Where melt temperature was not reported, we estimated it from the melt
272 composition (e.g., 950°C for andesitic magmas). Fig. 5 shows a strong relationship between
273 the amount of cooling and re-equilibration a gas has undergone and its oxidation state.

274

275 The observed decoupling between the oxidation states of volcanic gases and their melts
276 undermines the underlying assumption of gas-melt equilibrium in previous estimates of the
277 oxidation state of volcanic gases emitted in Earth's past or on other planets (e.g., Arculus and
278 Delano, 1980; Gaillard and Scaillet, 2014). It follows that variations in the oxidation state of
279 the Earth's mantle through time need not influence the oxidation state of volcanic gases emitted
280 to the atmosphere. Similarly, our observations imply that changes in geodynamic environment
281 on a global scale, such as from hotspot-dominated to arc-dominated volcanism, will not affect
282 the oxidation state of the volcanic gases emitted. Surficial processes, such as eruption style
283 should, however, influence the equilibrium and emission temperature of volcanic gases.
284 Explosive activity should always be associated with the emission of gases at lower temperature
285 and hence more oxidized gases as more closed-system cooling and expansion of the gas would
286 have taken place than during passive degassing. This can be seen, for instance, when comparing
287 passive and explosive gas emissions from Erebus volcano (Fig. 1 A) (Oppenheimer et al., 2011;
288 Burgisser et al., 2012).

289

290 The dependence of volcanic gas oxidation state on emission temperature helps to reconcile an
291 old paradox. Earth's atmosphere during the Archean was reduced (Bekker et al., 2004; Canfield
292 et al., 2000; Farquhar et al., 2007), and it has therefore been assumed that volcanic outgassing
293 was correspondingly more reduced (Holland, 2002; Kasting et al., 1993). Yet multiple lines of
294 evidence suggest that the Archean upper mantle and the melts it produced were as oxidised as
295 at present (e.g., Berry et al., 2008; Canil, 1997; Delano, 2001; Li and Lee, 2004) although this

296 conclusion has been disputed (e.g., Aulbach and Stagno, 2016; Nicklas et al., 2016)).
 297 Considering that the Archean was characterised by the eruption of komatiitic lava flows erupted
 298 at high temperatures of up to 1700°C (e.g., Huppert et al., 1984), the emission temperature of
 299 volcanic gases should have been considerably higher than at present. Extrapolating the data
 300 trend in Fig. 4 A and B, we suggest that volcanic gases emitted at ~1600 °C should have
 301 oxidation states between QFM–1 and QFM–2.5, even if the associated melt was more oxidized.
 302 These estimates are about one log unit more reduced than the average value of the hottest and
 303 most reduced gases emitted today, and at least two to three log units more reduced than the
 304 average volcanic gas emitted on Earth today (about QFM+1). We also note that the composition
 305 of these high-temperature gases should have been much richer in SO₂, H₂ and CO than today's
 306 volcanic emissions, e.g., SO₂/H₂S, H₂O/H₂ and CO₂/CO molar ratios of about 200, 20 and 2.5
 307 respectively at 1600°C, and 40, 120 and 60 at 1000°C (Fig. 6). The effect of these changes in
 308 gas composition on the oxidation state of the atmosphere can then be considered using
 309 Holland's criterion (f , defined as the fraction of sulfur in the initial volatiles that is converted
 310 to FeS₂, (Holland, 2002)):

$$311 \quad f = \frac{m_{H_2} + 0.6m_{CO} - 0.4m_{CO_2} + 3m_{H_2S}}{3.5(m_{SO_2} + m_{H_2S})} + \frac{1}{3.5} \quad (18)$$

312 Where m_i is the mole fraction of species i in the volcanic gas. If f exceeds 1 then the gas
 313 contains sufficient H₂ to reduce 20% of carbon gases to organic matter, and all sulfur to FeS₂.
 314 In other words, according to this criterion, a value of $f > 1$ corresponds to volcanic gases with
 315 the capacity to limit the accumulation of O₂ produced by oxygenic photosynthesis. Fig. 7 shows
 316 the relationship between f and gas equilibrium temperature for four starting gas compositions
 317 representing Erta 'Ale, Bromo, Satsuma Iwojima and Sabancaya volcanoes. Depending on the
 318 gas composition, the effect of emitting gases last equilibrated at 1400°C rather than 1000°C is
 319 equivalent to a 40–170% increase in f . Given that volcanic gases at present have average f
 320 values of 0.5 (Holland, 2002), f values of ~1 might have prevailed during the Archean. Similar

321 calculations for f based on the inferred gas composition for Mauna Kea (Brounce et al., 2017)
322 suggest that $f > 1$ would be attained for gas emitted at QFM-2.3, in broad agreement with our
323 calculations.

324

325 V. CONCLUSIONS

326 We have compiled a global dataset of volcanic gas measurements and demonstrated that,
327 relative to rock buffers, gas oxidation state is a strong function of emission temperature. With
328 decreasing temperature, gas oxidation state decreases by up to several orders of magnitude.
329 This trend is confirmed by two independent datasets, one based on measurements of volcanic
330 plumes whose constituent gases are diluted in air, the other synthesizing data from directly-
331 sampled gases emitted from high-temperature fumaroles.

332

333 We also find that neither geodynamic setting nor melt composition exerts an influence on the
334 oxidation state of the emitted gases. Together with a strong correlation between the gas
335 oxidation state and the difference between the melt and gas equilibrium temperatures, this
336 suggests that closed-system (gas-only) cooling of the gas is the process explaining our global
337 observations.

338

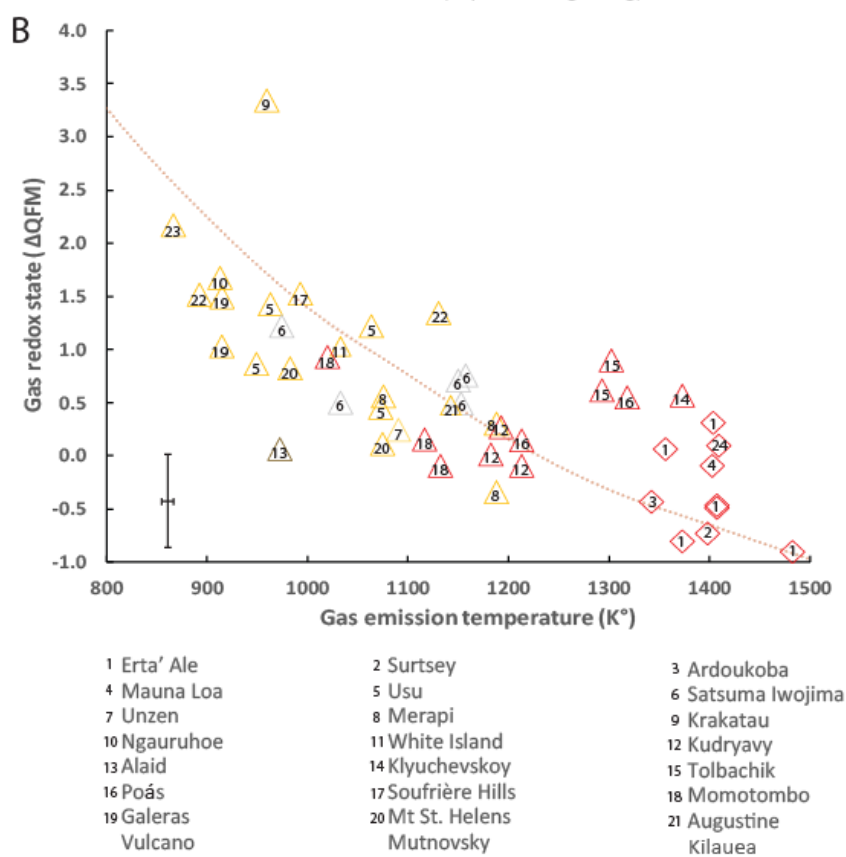
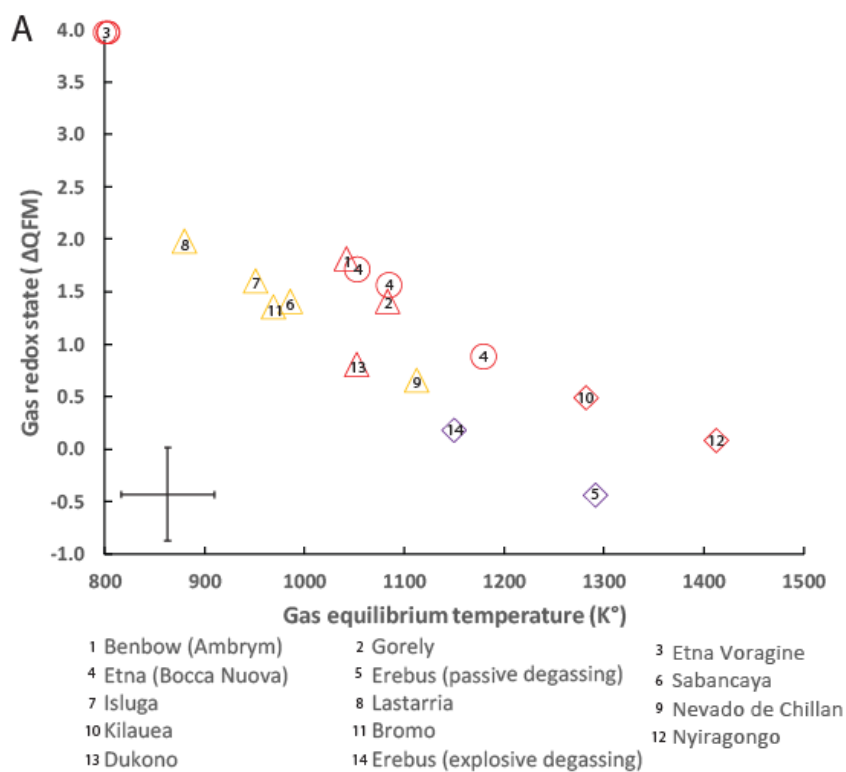
339 The observations enable us to estimate the mean oxidation state of volcanic gases emitted on
340 Earth at present to be approximately QFM+1.0. Extrapolation of our dataset suggests that the
341 equivalent figure for volcanic outgassing in the Archean was two to three log units more
342 reduced than today's average value.

343

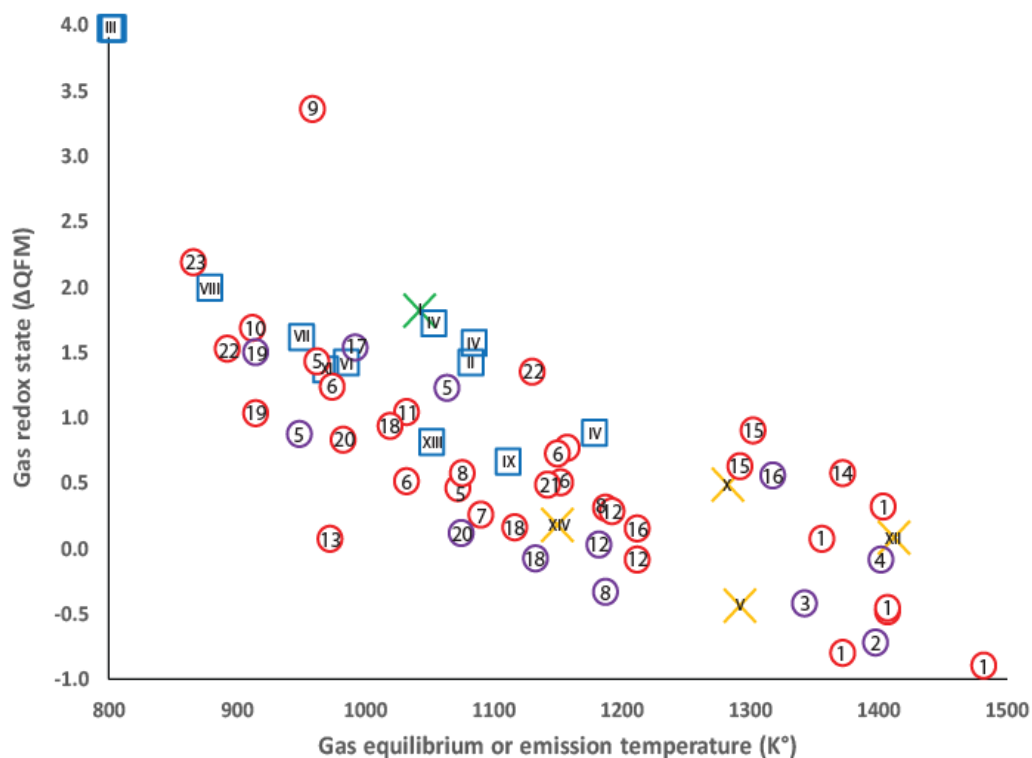
344 We further conclude that, globally, closed-system (gas-only) re-equilibration can have a
345 dramatic effect on the influence of gas emissions on the oxidation state of the atmosphere. The

346 cessation of widespread komatiitic volcanism between 2.5 and 2.0 Ga ago (e.g., Dostal, 2008)
347 should therefore have been accompanied by a shift towards more oxidised volcanic gas
348 emissions to the atmosphere, affecting the oxygen abundance in the atmosphere and oceans.
349 This evolution coincides with the major change in the oxidation state of the atmosphere during
350 the Paleo-Proterozoic, i.e., the Great Oxidation Event, 2.4 to 2.2 Ga ago (e.g., Canfield, 2005).
351 We suggest that decline of komatiitic volcanism likely facilitated this transition to an oxygen-
352 rich atmosphere, along with other proposed factors (Gaillard et al., 2011; Kump and Barley,
353 2007). Our results also show that relating volcanic gas redox states to their mantle source
354 cannot be made in any straightforward manner. Previous work has already shown that
355 decompression alone can significantly alter the redox signature of a magma relative to its
356 source (Moretti and Papale, 2004; Burgisser and Scaillet, 2007; Oppenheimer et al., 2011;
357 Gaillard and Scaillet, 2014; Moussallam et al., 2014, 2016). Our findings suggest further
358 complexity in this relationship by revealing a global relationship between gas emission
359 temperature and disequilibrium with respect to melt redox conditions.

360 FIGURES



362 **Figure 1: A.** Oxidation states of volcanic gases measured in air-diluted plumes (expressed as
363 deviations in log units from the QFM redox buffer) as a function of equilibrium temperature.
364 Triangles: arc volcanoes; diamonds: intraplate volcanoes; circles: Mt. Etna (whose origin is
365 debated). Red borders: volcanoes typically producing mafic magma; orange borders: volcanoes
366 associated with intermediate and silicic magmas (andesite to rhyolite); purple border: Mt.
367 Erebus, which erupts lavas of phonolitic composition. See **Supplementary Information** for
368 references. Note the strong negative correlation between gas equilibrium temperature and
369 oxidation state ($\Delta\text{QFM} = -0.0067T + 6.7097$ with an R^2 of 0.78 and a P-value of 1×10^{-6}). **B.**
370 Oxidation state (in log unit deviations from the QFM redox buffer) and measured emission
371 temperature of gas samples collected at accessible vents and analysed in the laboratory. Note
372 the strong negative correlation between gas emission temperature and oxidation state (ΔQFM
373 $= -0.0034T + 3.5536$ with an R^2 of 0.53 and a P-value of 5×10^{-9}). Representative error bars
374 are given. Brown dotted lines represent gas-only cooling trends calculated using gas
375 compositions reported for Erta 'Ale (Guern et al., 1979) volcano and solving for the reaction
376 $\text{SO}_2 + 3\text{H}_2 = \text{H}_2\text{S} + 2\text{H}_2\text{O}$ at 1 bar, using thermodynamic parameters given in Ohba et al.,
377 (1994).



Instrumental method

Multi-GAS: □

OP-FTIR: ×

Direct sampling: ○

Calculation method

$\text{H}_2/\text{H}_2\text{O}$ & $\text{H}_2\text{S}/\text{SO}_2$

CO/CO_2 & $\text{H}_2\text{S}/\text{SO}_2$

$\text{CO}_2\text{-CO-OCS-SO}_2$

$\text{H}_2/\text{H}_2\text{O}$ & T°

$\text{H}_2\text{S}/\text{SO}_2$ & T°

1 Erta' Ale

4 Mauna Loa

7 Unzen

10 Ngauruhoe

13 Alaid

16 Poás

19 Galeras

22 Vulcano

I Benbow (Ambrym)

IV Etna (Bocca Nuova)

VII Isluga

X Kilauea

XII Dukono

2 Surtsey

5 Usu

8 Merapi

11 White Island

14 Klyuchevskoy

17 Soufrière Hills

20 Mt St. Helens

23 Mutnovsky

II Gorely

V Erebus (passive degassing)

VIII Lastarria

XI Bromo

XV Erebus (explosive degassing)

3 Ardoukoba

6 Satsuma Iwojima

9 Krakatau

12 Kudryavy

15 Tolbachik

18 Momotombo

21 Augustine

III Etna Voragine

VI Sabancaya

IX Nevado de Chillan

XIII Nyiragongo

378

379 **Figure 2:** Oxidation state of volcanic gases as a function of emission or equilibrium

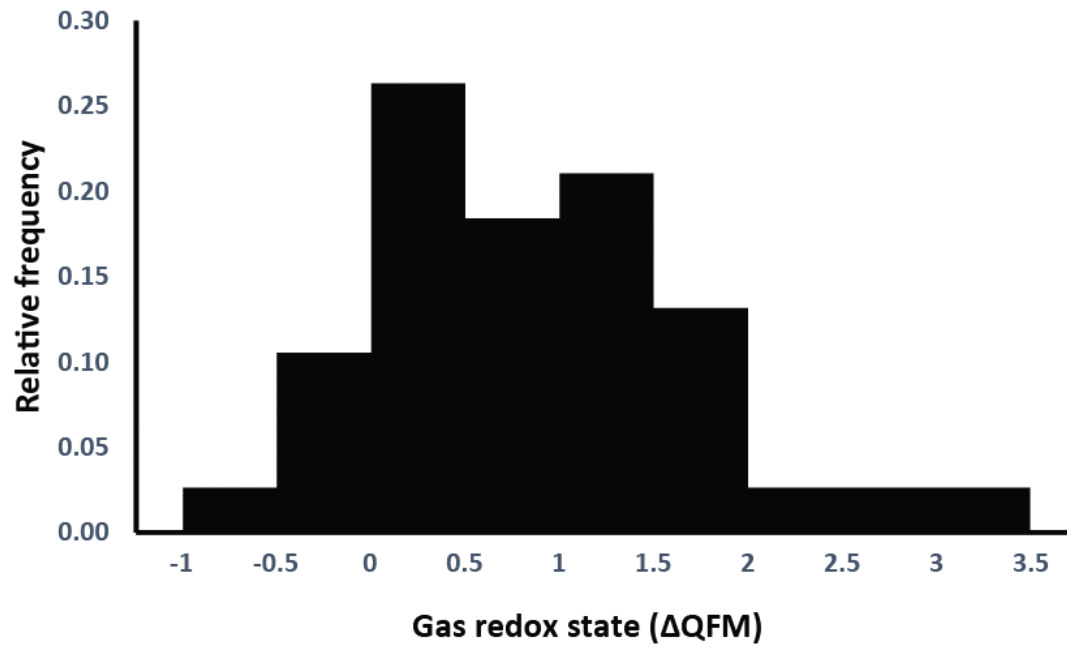
380 temperature for all high-temperature volcanic gases in our dataset, grouped by instrumental

381 method used to measure the gas composition (symbol shape) and by calculation method

382 (symbol colour) used to calculate the oxidation state and where applicable the equilibrium

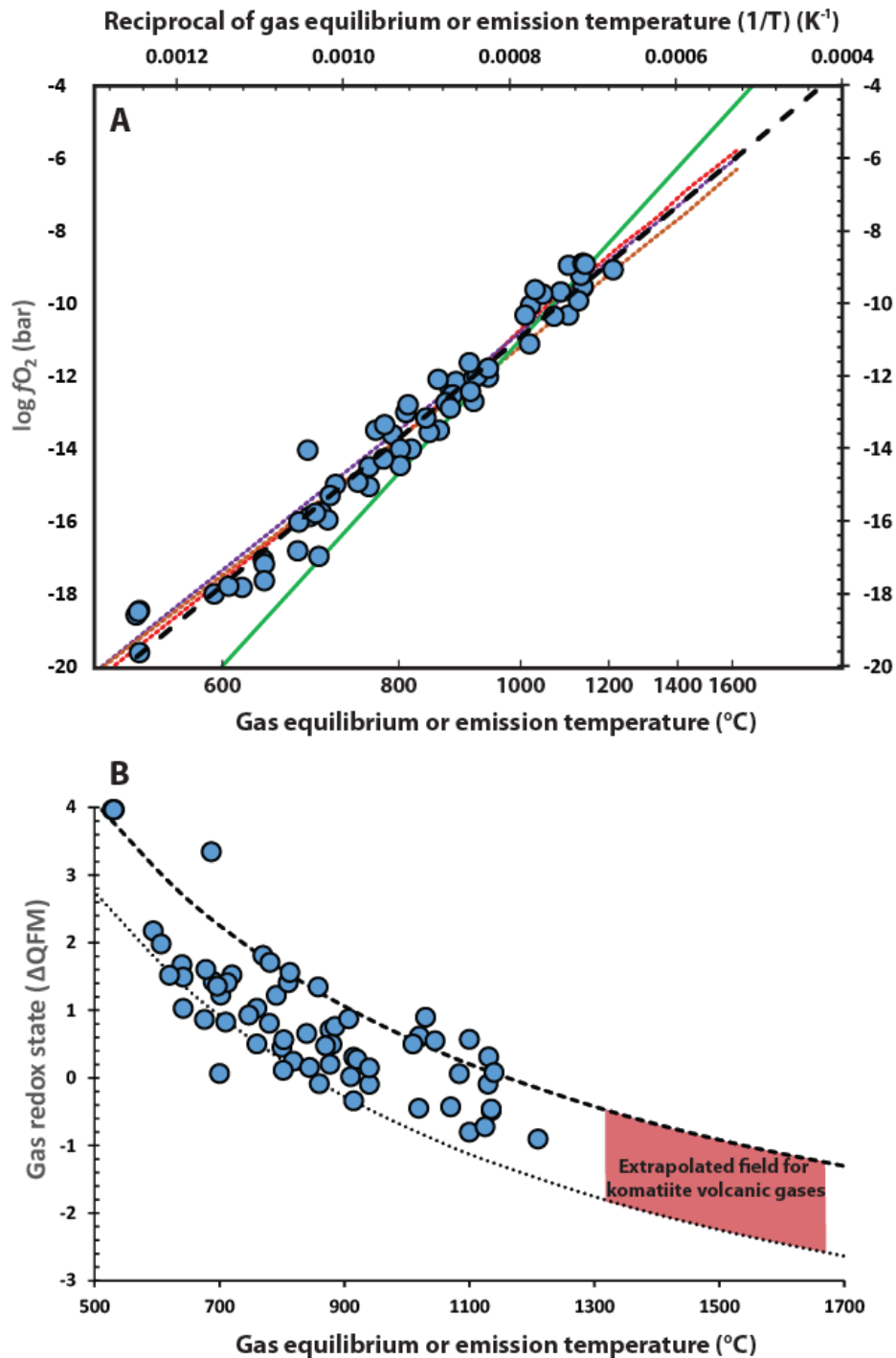
383 temperature.

384



385

386 **Figure 3:** Relative frequency distribution of the oxidation state of high-temperature volcanic
387 gases. The mean oxidation state of volcanic gases on Earth at present is about $\Delta QFM+1$.



388

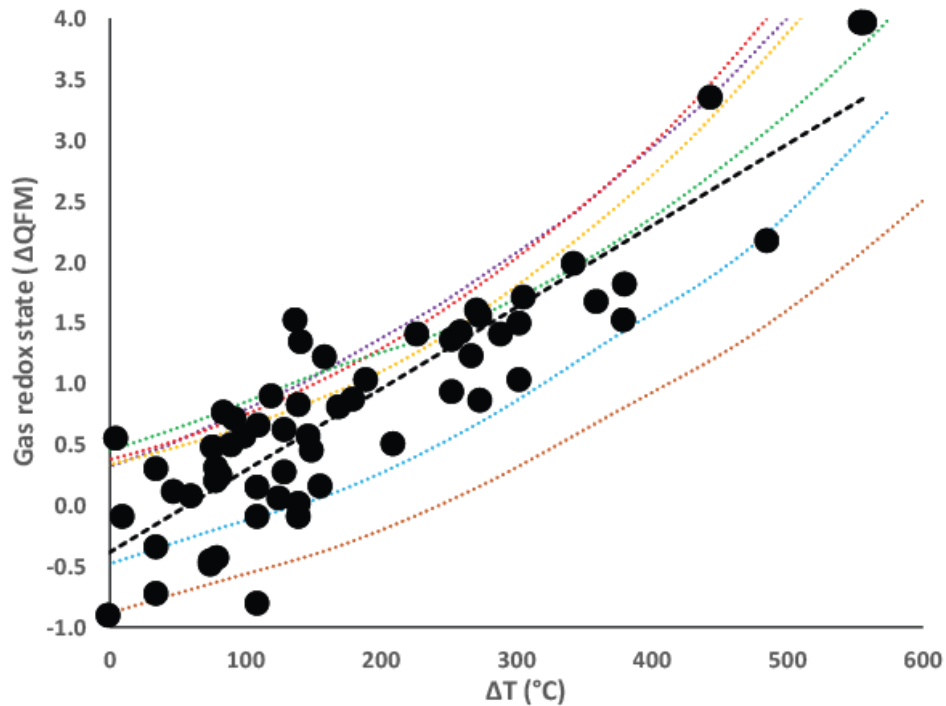
389 **Figure 4:** Oxidation state of volcanic gases as a function of emission or equilibrium

390 temperature for our combined dataset. A. Oxidation state expressed as oxygen fugacity. Green

391 line represents the QFM buffer, dashed black line represents a linear fit to the data ($\log f\text{O}_2 = -$ 392 $19093T + 4.081$ with $R^2=0.96$ and a P-value of 2×10^{-46}), red, purple and brown dotted lines

393 represent gas-only cooling trends calculated using gas compositions reported for Sabancaya

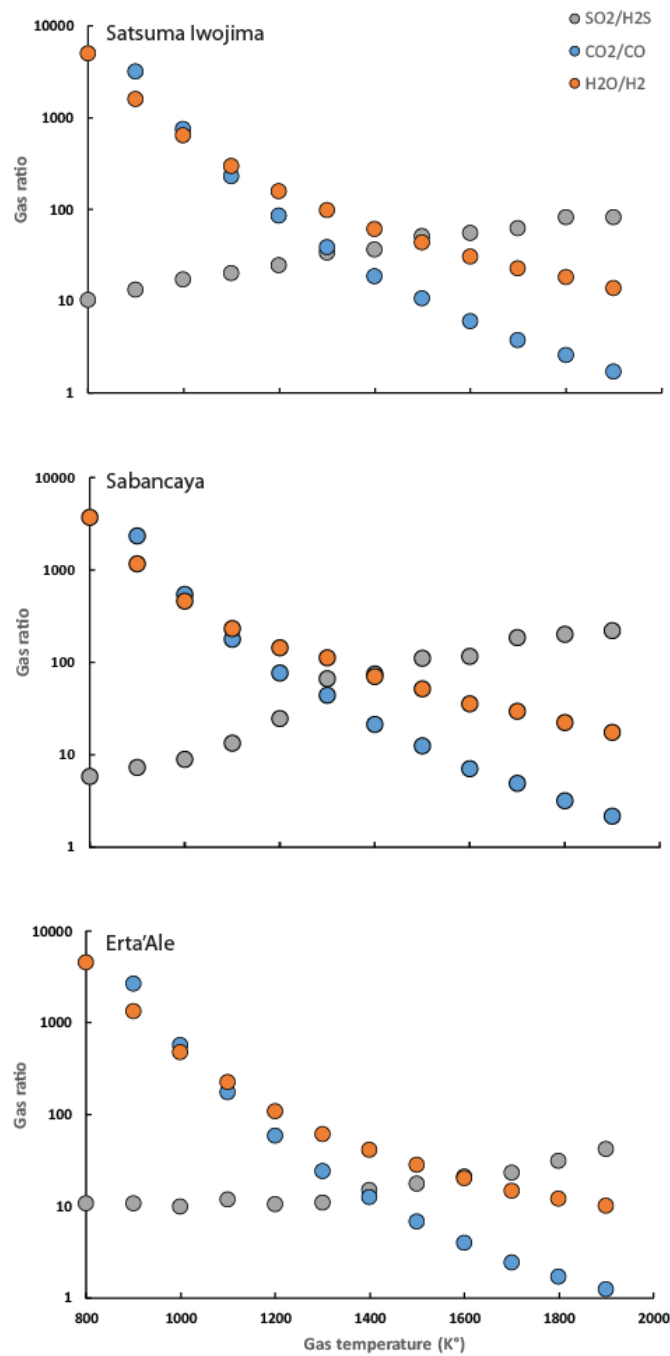
394 (Moussallam et al., 2017), Satsuma Iwojima (Goff and McMurtry, 2000) and Erta 'Ale (Guern
395 et al., 1979) volcanoes, respectively and solving for the reaction $\text{SO}_2 + 3\text{H}_2 = \text{H}_2\text{S} + 2\text{H}_2\text{O}$ at
396 1 bar, using thermodynamic parameters given in Ohba et al., (1994). Note the difference in
397 slope and intercept between the rock buffer and gas trend, and the close agreement between
398 global observations and closed-system cooling trends for three representative gas
399 compositions. **B.** Oxidation state expressed as deviation from the QFM buffer and temperature.
400 Dashed and dotted curves show the calculated relationship for a pure SO_2 - H_2S gas mixture
401 with $\text{SO}_2/\text{H}_2\text{S}$ ratio of 100 and 1, respectively. Trends are extrapolated to the higher
402 temperatures of komatiite lavas erupted during the Archean, suggesting even more reduced
403 conditions of the associated gas emissions to the atmosphere. Representative error bars are
404 given in Fig. 1.



405

406 **Figure 5:** Oxidation state of volcanic gases (expressed as deviation from the QFM buffer) as a
 407 function of the difference in gas emission or computed equilibrium temperature and the
 408 temperature of the associated melt. Dashed line is a linear regression through the data (ΔQFM
 409 $= -0.0068\Delta T + -0.4046$ with an R^2 of 0.8 and a P -value of 1×10^{-10}). Data and references are
 410 reported in [Table S3](#). Red, purple, brown, orange, green and blue dotted lines represent gas-
 411 only cooling trends calculated using gas compositions reported for Sabancaya (Moussallam et
 412 al., 2017), Satsuma Iwojima (Goff and McMurtry, 2000), Erta 'Ale (Guern et al., 1979), Bromo
 413 (Aiuppa et al., 2015), Etna (Aiuppa et al., 2011) and Momotombo (Giggenbach, 1996)
 414 volcanoes, respectively and solving for the reaction $\text{SO}_2 + 3\text{H}_2 = \text{H}_2\text{S} + 2\text{H}_2\text{O}$ at 1 bar, using
 415 thermodynamic parameters given in Ohba et al., (1994).

416



417

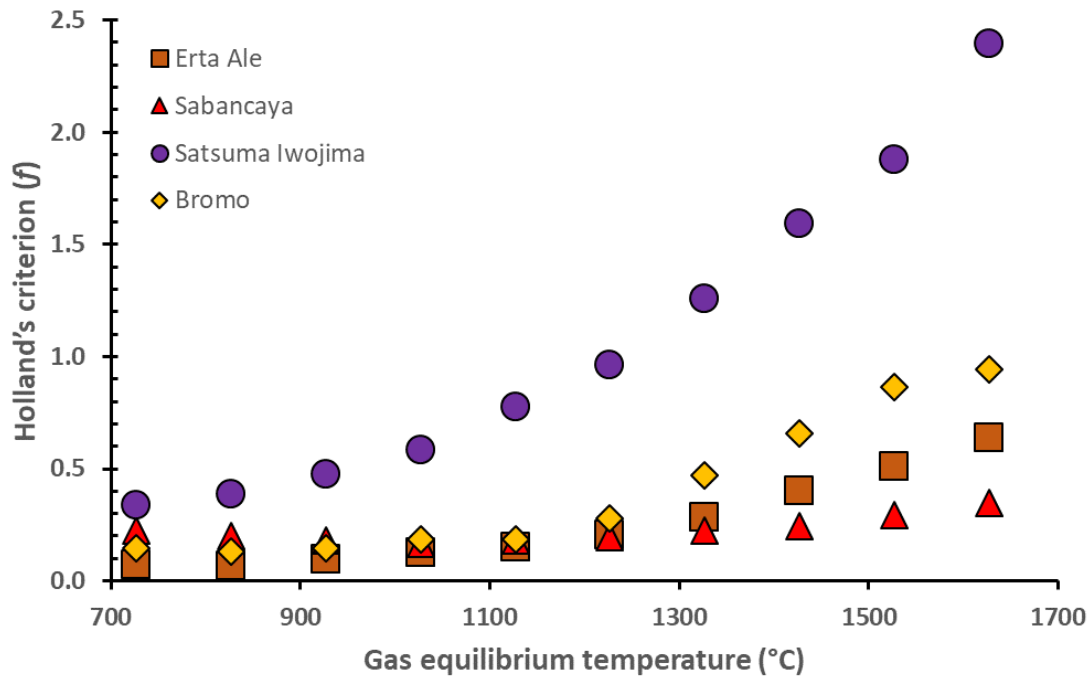
418 **Figure 6:** SO₂/H₂S; CO₂/CO and H₂O/H₂ gas ratios as a function of gas equilibrium

419 temperature. Gas compositions were calculated using compositional data for Sabancaya,

420 Satsuma Iwojima and Erta 'Ale volcanoes as representative starting points, and calculating the

421 equilibrium conditions for each gas mixture as a function of temperature from the equilibrium

422 $SO_2 + 3H_2 = H_2S + 2H_2O$ and using thermodynamic parameters given in Ohba et al., (1994).



423

424 **Figure 7:** Reducing capacity of volcanic gases, expressed as Holland's criterion, as a function

425 of gas equilibrium temperature. Reported gas compositions for Sabancaya (Moussallam et al.,

426 2017), Satsuma Iwojima (Goff and McMurtry, 2000), Erta 'Ale (Guern et al., 1979) and Bromo

427 (Aiuppa et al., 2015) are used in closed-system gas cooling calculations as shown in Fig. 4.

428 Note that, in all cases, increasing gas equilibrium temperature is accompanied by an increase

429 in Holland's criterion, demonstrating that the capacity of volcanic gases to reduce the

430 atmosphere increases as gas emission temperature increases.

431 REFERENCES

- 432 Aiuppa, A., Bani, P., Moussallam, Y., Di Napoli, R., Allard, P., Gunawan, H., Hendrasto, M.,
 433 Tamburello, G., 2015. First determination of magma-derived gas emissions from
 434 Bromo volcano, eastern Java (Indonesia). *J. Volcanol. Geotherm. Res.* 304, 206–213.
 435 <https://doi.org/10.1016/j.jvolgeores.2015.09.008>
- 436 Aiuppa, A., Shinohara, H., Tamburello, G., Giudice, G., Liuzzo, M., Moretti, R., 2011.
 437 Hydrogen in the gas plume of an open-vent volcano, Mount Etna, Italy. *J. Geophys.*
 438 *Res.* 116, 8 PP. <https://doi.org/201110.1029/2011JB008461>
- 439 Arculus, R.J., Delano, J.W., 1980. Implications for the primitive atmosphere of the oxidation
 440 state of Earth's upper mantle. *Nature* 288, 72–74. <https://doi.org/10.1038/288072a0>
- 441 Aulbach, S., Stagno, V., 2016. Evidence for a reducing Archean ambient mantle and its effects
 442 on the carbon cycle. *Geology* 44, 751–754. <https://doi.org/10.1130/G38070.1>
- 443 Bekker, A., Holland, H.D., Wang, P.-L., Rumble, D., Stein, H.J., Hannah, J.L., Coetzee, L.L.,
 444 Beukes, N.J., 2004. Dating the rise of atmospheric oxygen. *Nature* 427, 117–120.
 445 <https://doi.org/10.1038/nature02260>
- 446 Berry, A.J., Danyushevsky, L.V., O'Neill, H.S.C., Newville, M., Sutton, S.R., 2008. Oxidation
 447 state of iron in komatiitic melt inclusions indicates hot Archean mantle. *Nature* 455,
 448 960–963. <https://doi.org/10.1038/nature07377>
- 449 Brounce, M., Stolper, E., Eiler, J., 2017. Redox variations in Mauna Kea lavas, the oxygen
 450 fugacity of the Hawaiian plume, and the role of volcanic gases in Earth's oxygenation.
 451 *Proc. Natl. Acad. Sci.* 114, 8997–9002. <https://doi.org/10.1073/pnas.1619527114>
- 452 Burgisser, A., Oppenheimer, C., Alletti, M., Kyle, P., Scaillet, B., Carroll, M., 2012. Backward
 453 tracking of gas chemistry measurements at Erebus volcano. *Geochem. Geophys.*
 454 *Geosystems* 13.
- 455 Burgisser, A., Scaillet, B., 2007. Redox evolution of a degassing magma rising to the surface.
 456 *Nature* 445, 194–197.
- 457 Canfield, D.E., 2005. The early history of atmospheric oxygen: Homage to Robert M. Garrels.
 458 *Annu. Rev. Earth Planet. Sci.* 33, 1–36.
 459 <https://doi.org/10.1146/annurev.earth.33.092203.122711>
- 460 Canfield, D.E., Habicht, K.S., Thamdrup, B., 2000. The Archean Sulfur Cycle and the Early
 461 History of Atmospheric Oxygen. *Science* 288, 658–661.
 462 <https://doi.org/10.1126/science.288.5466.658>
- 463 Canil, D., 2002. Vanadium in peridotites, mantle redox and tectonic environments: Archean to
 464 present. *Earth Planet. Sci. Lett.* 195, 75–90. [https://doi.org/10.1016/S0012-821X\(01\)00582-9](https://doi.org/10.1016/S0012-821X(01)00582-9)
- 465 Canil, D., 1997. Vanadium partitioning and the oxidation state of Archean komatiite magmas.
 466 *Nature* 389, 842–845. <https://doi.org/10.1038/39860>
- 467 Carmichael, I.S., 1991. The redox states of basic and silicic magmas: a reflection of their
 468 source regions? *Contrib. Mineral. Petrol.* 106, 129–141.
 469 <https://doi.org/10.1007/BF00306429>
- 470 Carn, S.A., Fioletov, V.E., McLinden, C.A., Li, C., Krotkov, N.A., 2017. A decade of global
 471 volcanic SO₂ emissions measured from space. *Sci. Rep.* 7, 44095.
 472 <https://doi.org/10.1038/srep44095>
- 473 Chase, M.W., National Institute of Standards and Technology (U.S.), 1998. NIST-JANAF
 474 thermochemical tables. American Chemical Society ; American Institute of Physics for
 475 the National Institute of Standards and Technology, Washington, D.C.]; Woodbury,
 476 N.Y.

- 478 Chiodini, G., Marini, L., 1998. Hydrothermal gas equilibria: the H₂O-H₂-CO₂-CO-CH₄
479 system. *Geochim. Cosmochim. Acta* 62, 2673–2687. <https://doi.org/10.1016/S0016->
480 7037(98)00181-1
- 481 Delano, J.W., 2001. Redox history of the Earth's interior since approximately 3900 Ma:
482 implications for prebiotic molecules. *Orig. Life Evol. Biosphere J. Int. Soc. Study Orig.*
483 *Life* 31, 311–341.
- 484 Dostal, J., 2008. Igneous Rock Associations 10. Komatiites. *Geosci. Can.* 35.
- 485 Elkins-Tanton, L.T., 2008. Linked magma ocean solidification and atmospheric growth for
486 Earth and Mars. *Earth Planet. Sci. Lett.* 271, 181–191.
487 <https://doi.org/10.1016/j.epsl.2008.03.062>
- 488 Farquhar, J., Peters, M., Johnston, D.T., Strauss, H., Masterson, A., Wiechert, U., Kaufman,
489 A.J., 2007. Isotopic evidence for Mesoarchean anoxia and changing atmospheric
490 sulphur chemistry. *Nature* 449, 706–709. <https://doi.org/10.1038/nature06202>
- 491 Frost, B.R., 1991. Introduction to oxygen fugacity and its petrologic importance. *Rev. Mineral.*
492 *Geochem.* 25, 1–9.
- 493 Frost, D.J., McCammon, C.A., 2008. The Redox State of Earth's Mantle. *Annu. Rev. Earth*
494 *Planet. Sci.* 36, 389–420. <https://doi.org/10.1146/annurev.earth.36.031207.124322>
- 495 Gaillard, F., Scaillet, B., 2014. A theoretical framework for volcanic degassing chemistry in a
496 comparative planetology perspective and implications for planetary atmospheres. *Earth*
497 *Planet. Sci. Lett.* 403, 307–316. <https://doi.org/10.1016/j.epsl.2014.07.009>
- 498 Gaillard, F., Scaillet, B., Arndt, N.T., 2011. Atmospheric oxygenation caused by a change in
499 volcanic degassing pressure. *Nature* 478, 229–232.
500 <https://doi.org/10.1038/nature10460>
- 501 Gerlach, T.M., 2004. Volcanic sources of tropospheric ozone-depleting trace gases. *Geochem.*
502 *Geophys. Geosystems* 5, n/a–n/a. <https://doi.org/10.1029/2004GC000747>
- 503 Gerlach, T.M., 1993. Oxygen buffering of Kilauea volcanic gases and the oxygen fugacity of
504 Kilauea basalt 795–814.
- 505 Giggenbach, W., 1996. Chemical composition of volcanic gases. Scarpa R Tilling RI Eds
506 *Monit. Mitig. Volcano Hazards* 202–226.
- 507 Giggenbach, W.F., 1996. Chemical Composition of Volcanic Gases, in: *Monitoring and*
508 *Mitigation of Volcano Hazards*. Springer Berlin Heidelberg, pp. 221–256.
509 https://doi.org/10.1007/978-3-642-80087-0_7
- 510 Giggenbach, W.F., 1987. Redox processes governing the chemistry of fumarolic gas discharges
511 from White Island, New Zealand. *Appl. Geochem.* 2, 143–161.
512 [https://doi.org/10.1016/0883-2927\(87\)90030-8](https://doi.org/10.1016/0883-2927(87)90030-8)
- 513 Giggenbach, W.F., 1980. Geothermal gas equilibria. *Geochim. Cosmochim. Acta* 44, 2021–
514 2032. [https://doi.org/10.1016/0016-7037\(80\)90200-8](https://doi.org/10.1016/0016-7037(80)90200-8)
- 515 Giggenbach, W.F., Tedesco, D., Sulistiyo, Y., Caprai, A., Cioni, R., Favara, R., Fischer, T.P.,
516 Hirabayashi, J.-I., Korzhinsky, M., Martini, M., Menyailov, I., Shinohara, H., 2001.
517 Evaluation of results from the fourth and fifth IAVCEI field workshops on volcanic
518 gases, Vulcano island, Italy and Java, Indonesia. *J. Volcanol. Geotherm. Res.* 108, 157–
519 172. [https://doi.org/10.1016/S0377-0273\(00\)00283-3](https://doi.org/10.1016/S0377-0273(00)00283-3)
- 520 Goff, F., McMurtry, G.M., 2000. Tritium and stable isotopes of magmatic waters. *J. Volcanol.*
521 *Geotherm. Res.* 97, 347–396. [https://doi.org/10.1016/S0377-0273\(99\)00177-8](https://doi.org/10.1016/S0377-0273(99)00177-8)
- 522 Guern, F.L., Carbonnelle, J., Tazieff, H., 1979. Erta'ale lava lake: heat and gas transfer to the
523 atmosphere. *J. Volcanol. Geotherm. Res.* 6, 27–48. <https://doi.org/10.1016/0377->
524 0273(79)90045-3
- 525 Halevy, I., Johnston, D.T., Schrag, D.P., 2010. Explaining the Structure of the Archean Mass-
526 Independent Sulfur Isotope Record. *Science* 329, 204–207.
527 <https://doi.org/10.1126/science.1190298>

- 528 Hirschmann, M.M., Dasgupta, R., 2009. The H/C ratios of Earth's near-surface and deep
529 reservoirs, and consequences for deep Earth volatile cycles. *Chem. Geol., Volatiles and*
530 *Volatile-Bearing Melts in the Earth's Interior* 262, 4–16.
531 <https://doi.org/10.1016/j.chemgeo.2009.02.008>
- 532 Holland, H., 2002. Volcanic gases, black smokers, and the great oxidation event. *Geochim.*
533 *Cosmochim. Acta* 66, 3811–3826. [https://doi.org/10.1016/S0016-7037\(02\)00950-X](https://doi.org/10.1016/S0016-7037(02)00950-X)
- 534 Huppert, H.E., Sparks, R.S.J., Turner, J.S., Arndt, N.T., 1984. Emplacement and cooling of
535 komatiite lavas. *Nature* 309, 19–22. <https://doi.org/10.1038/309019a0>
- 536 Kasting, J., Egger, D., Raeburn, S., 1993. Mantle Redox Evolution and the Oxidation State
537 of the Archean Atmosphere. *J. Geol.* 101, 245–257.
- 538 Kasting, J.F., 1993. Earth's early atmosphere. *Science* 259, 920–926.
- 539 Kasting, J.F., and, Catling, D., 2003. Evolution of a Habitable Planet. *Annu. Rev. Astron.*
540 *Astrophys.* 41, 429–463. <https://doi.org/10.1146/annurev.astro.41.071601.170049>
- 541 Kump, L.R., Barley, M.E., 2007. Increased subaerial volcanism and the rise of atmospheric
542 oxygen 2.5 billion years ago. *Nature* 448, 1033–1036.
543 <https://doi.org/10.1038/nature06058>
- 544 Li, Z., Lee, C., 2004. The constancy of upper mantle fO₂ through time inferred from V/Sc
545 ratios in basalts. *Earth Planet. Sci. Lett.* 228, 483–493.
546 <https://doi.org/10.1016/j.epsl.2004.10.006>
- 547 Martin, R.S., Mather, T.A., Pyle, D.M., 2006. High-temperature mixtures of magmatic and
548 atmospheric gases. *Geochem. Geophys. Geosystems* 7.
- 549 Martin, R.S., Roberts, T.J., Mather, T.A., Pyle, D.M., 2009. The implications of H₂S and H₂
550 kinetic stability in high-T mixtures of magmatic and atmospheric gases for the
551 production of oxidized trace species (e.g., BrO and NO_x). *Chem. Geol.* 263, 143–150.
552 <https://doi.org/10.1016/j.chemgeo.2008.12.028>
- 553 Moretti, R., Ottonello, G., 2005. Solubility and speciation of sulfur in silicate melts: The
554 Conjugated Toop-Samis-Flood-Grjotheim (CTSFG) model. *Geochim. Cosmochim.*
555 *Acta* 69, 801–823. <https://doi.org/10.1016/j.gca.2004.09.006>
- 556 Moretti, R., Papale, P., 2004. On the oxidation state and volatile behavior in multicomponent
557 gas-melt equilibria. *Chem. Geol.* 213, 265–280.
558 <https://doi.org/10.1016/j.chemgeo.2004.08.048>
- 559 Moretti, R., Papale, P., Ottonello, G., 2003. A model for the saturation of C-O-H-S fluids in
560 silicate melts. *Geol. Soc. Lond. Spec. Publ.* 213, 81–101.
561 <https://doi.org/10.1144/GSL.SP.2003.213.01.06>
- 562 Mori, T., Notsu, K., Tohjima, Y., Wakita, H., 1993. Remote detection of HCl and SO₂ in
563 volcanic gas from Unzen volcano, Japan. *Geophys. Res. Lett.* 20, 1355–1358.
564 <https://doi.org/10.1029/93GL01065>
- 565 Moussallam, Y., Bani, P., Schipper, C.I., Cardona, C., Franco, L., Barnie, T., Amigo, Á.,
566 Curtis, A., Peters, N., Aiuppa, A., Giudice, G., Oppenheimer, C., 2018. Unrest at the
567 Nevados de Chillán volcanic complex: a failed or yet to unfold magmatic eruption?
568 *Volcanica* 1, 19–32. <https://doi.org/10.30909/vol.01.01.1932>
- 569 Moussallam, Y., Edmonds, M., Scaillet, B., Peters, N., Gennaro, E., Sides, I., Oppenheimer,
570 C., 2016. The impact of degassing on the oxidation state of basaltic magmas: A case
571 study of Kilauea volcano. *Earth Planet. Sci. Lett.* 450, 317–325.
572 <https://doi.org/10.1016/j.epsl.2016.06.031>
- 573 Moussallam, Y., Oppenheimer, C., Scaillet, B., Gaillard, F., Kyle, P., Peters, N., Hartley, M.,
574 Berlo, K., Donovan, A., 2014. Tracking the changing oxidation state of Erebus
575 magmas, from mantle to surface, driven by magma ascent and degassing. *Earth Planet.*
576 *Sci. Lett.* 393, 200–209. <https://doi.org/10.1016/j.epsl.2014.02.055>

- 577 Moussallam, Y., Tamburello, G., Peters, N., Apaza, F., Schipper, C.I., Curtis, A., Aiuppa, A.,
 578 Masias, P., Boichu, M., Bauduin, S., Barnie, T., Bani, P., Giudice, G., Moussallam, M.,
 579 2017. Volcanic gas emissions and degassing dynamics at Ubinas and Sabancaya
 580 volcanoes; implications for the volatile budget of the central volcanic zone. *J. Volcanol.*
 581 *Geotherm. Res.* <https://doi.org/10.1016/j.jvolgeores.2017.06.027>
- 582 Nicklas, R.W., Puchtel, I.S., Ash, R.D., 2016. High-precision determination of the oxidation
 583 state of komatiite lavas using vanadium liquid-mineral partitioning. *Chem. Geol.* 433,
 584 36–45. <https://doi.org/10.1016/j.chemgeo.2016.04.011>
- 585 Ohba, T., Hirabayashi, J., Yoshida, M., 1994. Equilibrium temperature and redox state of
 586 volcanic gas at Unzen volcano, Japan. *J. Volcanol. Geotherm. Res.* 60, 263–272.
 587 [https://doi.org/10.1016/0377-0273\(94\)90055-8](https://doi.org/10.1016/0377-0273(94)90055-8)
- 588 Oppenheimer, C., Moretti, R., Kyle, P.R., Eschenbacher, A., Lowenstern, J.B., Hervig, R.L.,
 589 Dunbar, N.W., 2011. Mantle to surface degassing of alkalic magmas at Erebus volcano,
 590 Antarctica. *Earth Planet. Sci. Lett.* 306, 261–271.
 591 <https://doi.org/10.1016/j.epsl.2011.04.005>
- 592 Oppenheimer, C., Scaillet, B., Woods, A., Sutton, A.J., Elias, T., Moussallam, Y., 2018.
 593 Influence of eruptive style on volcanic gas emission chemistry and temperature. *Nat.*
 594 *Geosci.* 1. <https://doi.org/10.1038/s41561-018-0194-5>
- 595 Ottonello, G., Moretti, R., Marini, L., Vetuschi Zuccolini, M., 2001. Oxidation state of iron in
 596 silicate glasses and melts: a thermochemical model. *Chem. Geol.*, 6th International
 597 Silicate Melt Workshop 174, 157–179. [https://doi.org/10.1016/S0009-2541\(00\)00314-](https://doi.org/10.1016/S0009-2541(00)00314-4)
 598 4
- 599 Peters, N., Oppenheimer, C., Killingsworth, D.R., Frechette, J., Kyle, P., 2014. Correlation of
 600 cycles in Lava Lake motion and degassing at Erebus Volcano, Antarctica. *Geochem.*
 601 *Geophys. Geosystems* 15, 3244–3257. <https://doi.org/10.1002/2014GC005399>
- 602 Rollinson, H., Adetunji, J., Lenaz, D., Szilas, K., 2017. Archaean chromitites show constant
 603 Fe³⁺/ΣFe in Earth's asthenospheric mantle since 3.8Ga. *Lithos* 282, 316–325.
 604 <https://doi.org/10.1016/j.lithos.2017.03.020>
- 605 Shinohara, H., 2013. Volatile flux from subduction zone volcanoes: Insights from a detailed
 606 evaluation of the fluxes from volcanoes in Japan. *J. Volcanol. Geotherm. Res.* 268, 46–
 607 63. <https://doi.org/10.1016/j.jvolgeores.2013.10.007>
- 608 Shinohara, H., 2005. A new technique to estimate volcanic gas composition: plume
 609 measurements with a portable multi-sensor system. *J. Volcanol. Geotherm. Res.* 143,
 610 319–333. <https://doi.org/10.1016/j.jvolgeores.2004.12.004>
- 611 Stull, D.R., Westrum, E.F., Sinke, G.C., 1969. The chemical thermodynamics of organic
 612 compounds. J. Wiley.
- 613 Symonds, R.B., Gerlach, T.M., Reed, M.H., 2001. Magmatic gas scrubbing: implications for
 614 volcano monitoring. *J. Volcanol. Geotherm. Res.* 108, 303–341.
 615 [https://doi.org/10.1016/S0377-0273\(00\)00292-4](https://doi.org/10.1016/S0377-0273(00)00292-4)
- 616 Symonds, R.B., Rose, W.I., Bluth, G.J.S., Gerlach, T.M., 1994. Volcanic-gas studies; methods,
 617 results, and applications. *Rev. Mineral. Geochem.* 30, 1–66. [https://doi.org/10.1016/S0377-0273\(94\)00001-0](https://doi.org/10.1016/S0377-0273(94)00001-0)

618 ACKNOWLEDGEMENTS

- 619 Y.M. acknowledges support from the Leverhulme Trust. CO receives support from the NERC
 620 Centre for Observation and Modelling of Earthquakes, Volcanoes and Tectonics and NERC

621 grant NE/N009312/1. We thank Dr. Roberto Moretti and anonymous referees for constructive
622 and beneficial comments on the original manuscript.